Critical parameters sensitivity analysis in thermal modeling of permafrost ground response to climate warming

Khatereh Roghangar, Jocelyn L. Hayley
University of Calgary, Calgary, Alberta, Canada
Department of Civil Engineering – University of Calgary, Calgary, Alberta, Canada

ABSTRACT
Climate change has had a significant impact on the Arctic region over the past few decades, where it poses a threat to the stability of permafrost bringing increased temperatures and changes in weather. The harmonic active layer has been shown to be impacted by climate change at the ground surface, and warmer air temperatures can result in progressive permafrost thaw, resulting in a deeper active layer. This study aims to assess the effects of critical parameters on the response of permafrost ground to climate warming using the fifth phase of the Coupled Model Intercomparison Project (CMIP5). We used TEMP/W to predict the depth of the active layer in the future by analyzing variations in depth, water content, and soil types. The results indicate that, for fine-grained soils, the depth of the model is a more significant parameter than for course-grained soils. The water content of all soil types is a critical factor in determining the time at which permafrost disappears or the depth at which the active layer is located. There is a significant difference in results when using different climate models for samples containing less water at lower depths.

RÉSUMÉ
Le changement climatique a eu un impact significatif sur la région arctique au cours des dernières décennies, où il constitue une menace pour la stabilité du pergélisol en raison de l'augmentation des températures et des changements météorologiques. Il a été démontré que la couche active harmonique est affectée par le changement climatique à la surface du sol, et que des températures de l'air plus élevées peuvent entraîner un dégel progressif du pergélisol, ce qui se traduit par une couche active plus profonde. Cette étude vise à évaluer les effets des paramètres critiques sur la réponse du sol pergélisol au réchauffement climatique en utilisant la cinquième phase du Projet de comparaison de modèles couplés (CMIP5). Nous avons utilisé TEMP/W pour prédire la profondeur de la couche active à l'avenir en analysant les variations de la profondeur, de la teneur en eau et des types de sol. Les résultats indiquent que, pour les sols à grain fin, la profondeur du modèle est un paramètre plus important que pour les sols à grain grossier. La teneur en eau de tous les types de sol est un facteur essentiel pour déterminer le moment où le pergélisol disparaît ou la profondeur à laquelle se trouve la couche active. L'utilisation de différents modèles climatiques permet d'obtenir des résultats très différents pour les échantillons contenant moins d'eau à des profondeurs moindres.

1. INTRODUCTION

Permafrost refers to soil or rock that has been below 0℃ for at least two consecutive years and is primarily influenced by climate. The percentage of permafrost-covered area and thickness tends to increase as air temperatures decrease farther northward (Canadian Standards Association, 2019).

Arctic landscapes are rapidly changing due to climate change, which could cause almost 5°C of warming by 2100 according to the IPCC (IPCC, 2014). The resulting thawing of permafrost could lead to thickening of the active layer and widespread thaw settlement. To design and build Arctic infrastructure, it is necessary to understand and examine current and future climate conditions, as most existing infrastructures were not designed with climate change in mind (Roghani, 2021; Sadollahzadeh et al., 2021; Vahdani et al., 2022).

This study examines the site characteristics of the Hudson Bay Railway (HBR) regions, which were built on permafrost in the 1920s. A thermal model is used to simulate the effects of air temperature predictions on the near-surface ground thermal regime, and a sensitivity analysis of water content amount of soil and depth of model on the thickness and settlement of the active layer is presented. This research aims to assess the impact of permafrost degradation due to climate warming on the performance of infrastructure embankment.

2. CLIMATE DATA

In order to understand climatic conditions and how they are projected to change in the future, we collected the daily maximum and minimum air temperatures from Climate Data Canada for three stations along the HBR that were chosen based on the three permafrost zones (continuous, extensive discontinuous, and sporadic discontinuous). For our analysis, we selected the GFDL-ESM2G climate model. Figure 1 illustrates the study area and each station for deriving the air temperature data. Figure 2 illustrates the average daily air temperature for three climate scenarios (RCP2.6, RCP4.5, and RCP8.5) at the selected stations.

Figure 1. The study area and the location of the stations in each permafrost zone.

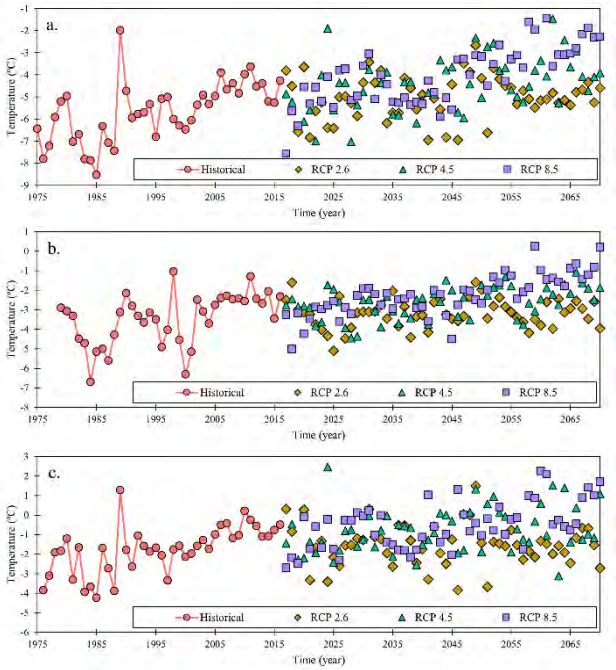

Figure 2. Historical and projected daily air temperatures at the a. Churchill Station, in the continuous permafrost zone (Jan. 1975 - Jan. 2070), b. Charlebois Station, in the extensive discontinuous permafrost zone (Jan. 1979 - Jan. 2070) and c. Sipiwesk Station, in the sporadic discontinuous permafrost zone (Sep. 1976 - Sep. 2070).

3. THERMAL MODELING

To simulate the soil profile conditions and changes beneath the road embankment along the HBR, we constructed a geothermal model. Our numerical model was created using the commercial computer software TEMP/W, which is a component of the geotechnical software package GeoStudio (GeoSlope, 2021). The software utilizes a two-dimensional finite element method of analysis to compute thermal distributions in the ground. The governing differential equation used in the analysis is

$$\frac{\partial}{\partial x}\left(k_x \frac{\partial T}{\partial x}\right) + \frac{\partial}{\partial y}\left(k_y \frac{\partial T}{\partial y}\right) + Q = \lambda \frac{\partial T}{\partial t} \quad [1]$$

where T=temperature (℃); k_x=thermal conductivity in the x direction (J/s/m/ºC); k_y=thermal conductivity in the y direction (J/s/m/ºC); Q=applied boundary flux (mW/m2); λ=capacity for heat storage (kJ/m3/ºC); and t=time (s). The capacity for heat storage can be expressed as

$$\lambda = c + L\Theta \frac{\partial \Theta_u}{\partial T} \quad [2]$$

where c is the volumetric heat capacity at frozen and unfrozen temperatures (kJ/m3/ºC). The second term depends on the latent heat L of water (J/kg), the volumetric water content Θ, and the change in unfrozen water content of the soil with temperature (∂Θ)/∂T. It represents the amount of heat released of absorbed as the temperature of the soil changes by ∂T. Equation 2 can be substituted in Equation 1 to get the following equation:

$$\frac{\partial}{\partial x}\left(k_x \frac{\partial T}{\partial x}\right) + \frac{\partial}{\partial y}\left(k_y \frac{\partial T}{\partial y}\right) + Q = \left(c + L\Theta \frac{\partial \Theta_u}{\partial T}\right) \frac{\partial T}{\partial t} \quad [3]$$

To incorporate temperature variations in a transient analysis, Equation 3 is implemented for every node in the model domain.

3.1 Model Geometry and Boundary Conditions

In this study, we selected five soil types for the purpose of evaluating their response to climate warming. Consequently, the thermal modeling was targeted towards five distinct 50m soil columns, each representing a different soil type based on the EBA Engineering Ltd.'s reports (EBA Engineering Consultants Ltd., 1977; EBA Engineering Consultants Ltd., 1975). Figure 3 depicts the models, including the constituent elements and boundary conditions.

There are two vertical non-flux boundaries at the sides of the model, a constant heat flux boundary at the bottom of the model, and an upper boundary condition that depends on empirical factors, such as the type of material, snow cover, vegetation cover and the air temperature (Figure 3). Non-flux boundary conditions apply to both sides of the model as they represent undisturbed conditions, and they will not affect the model's results. In this study, we evaluated three options for bottom boundary conditions: 1. Setting heat flux, 2. Applying infinite elements along the boundary and 3. Setting a fixed temperature. While the first and third options offered better computational cost, the second option provided more realistic conditions (Alfaro et al., 2009). Ultimately, we selected a constant heat flux as the bottom boundary condition and derived the appropriate heat flux values from the Global Heat Flow Database. For the continuous, extensive discontinuous, and sporadic discontinuous permafrost models, we applied heat flux values of 30.3, 51.7, and 47.9 mW/m2, respectively.

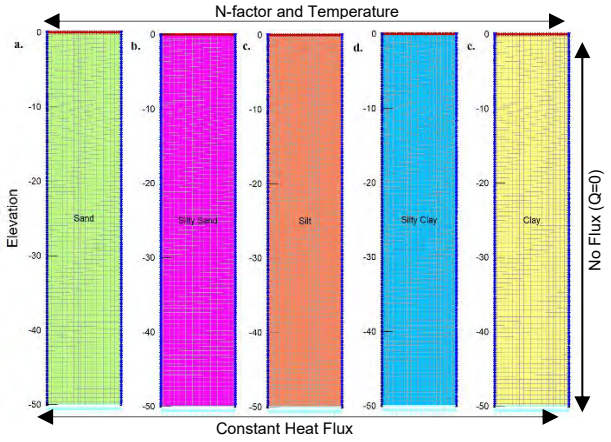

Figure 3. Material, boundary conditions and mesh for 5 modeling setups for a. sand, b. silty sand, c. silt, d. silty clay and e. clay material.

In our thermal modeling using TEMP/W, we evaluated two different approaches for calculating ground surface temperature at the upper boundary: the surface energy balance method and the use of n factors. The surface energy balance method, while more accurate, requires a vast amount of data including maximum and minimum temperature, relative humidity, wind speed, precipitation amounts and timing, latitude, longitude, maximum snow temperature, and minimum rain temperature. However, we were unable to use this approach in our model due to the difficulty of obtaining reliable model parameters for the future 50-year analysis period or even for the present. Instead, we adopted the empirical approach of using n factors and air temperature as boundary modifiers, which provided a feasible and reasonable solution. The n factor for freezing, n_f, and thawing, n_t, are defined as the ratio of the surface freezing or thawing index (I_{sf} and I_{st}) to the air freezing or thawing index (I_{af} and I_{at}) as described in the following equations (Lunardini, 1978)

$$n_f = \frac{I_{sf}}{I_{af}} \quad [4]$$

$$n_t = \frac{I_{st}}{I_{at}} \quad [5]$$

The air freezing index and air thawing index are important parameters used to quantify the freezing and thawing conditions in a given area. The air freezing index is defined as the cumulative number of freezing or negative degree days between the maximum and minimum points on the curve of accumulative freezing degree days versus time from the onset of freezing temperatures. Freezing degree days, on the other hand, are defined as the absolute value of the mean air temperature when it is below freezing. Similarly, the air thawing index is the cumulative number of positive or thawing degree days between the maximum in spring and the minimum in autumn (Andersland & Ladanyi, 2004).

The values of n factors used in the TEMP/W model depend on the surface type and climatic and hydrological conditions. These values are available in the literature for a range of conditions. For this study, the n factor values of 0.9 and 2 were used for sand and gravel surface condition for freezing and thawing conditions, respectively (Andersland & Ladanyi, 2004). It is assumed that the surface condition is sand and gravel and no vegetation exists.

3.2 Initial Conditions

In our analysis, the more advanced option of specifying initial temperature conditions in TEMP/W was utilized, which involves using the results of a steady-state model as the initial conditions for the transient analysis. This option is considered more advanced as it allows for a more accurate representation of the initial temperature conditions in the numerical model. In contrast, the standard option involves manually applying initial temperatures to each individual node, which may not accurately capture the actual initial temperature distribution in the ground.

In this study, the thermistor data for each station was obtained from HBR reports (EBA Engineering Consultants Ltd., 1977) for discontinuous permafrost and from the Polar Gas Pipeline reports (EBA Engineering Consultants Ltd., 1975) for continuous permafrost from different sites. Figure 4 illustrates the initial condition graphs that were utilized for the steady-state analysis. It is important to mention that the initial conditions for the continuous, extensive discontinuous, and sporadic discontinuous permafrost stations were based on 1, 15, and 2 number of data sets, respectively, retrieved from the relevant databases. When multiple data sets were available, the mean value was used to determine the initial condition. As the initial condition for each permafrost types is in a different season, the time steps is the modeling is adjusted accordingly.

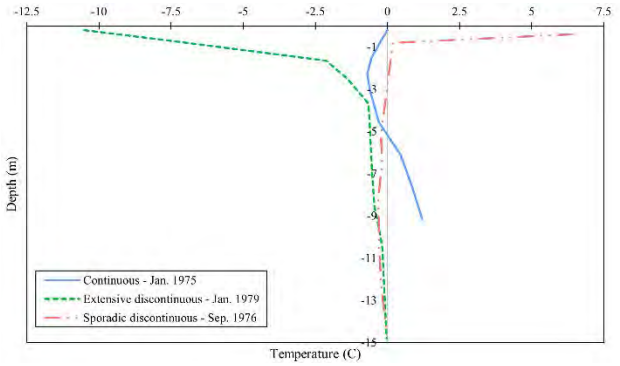

Figure 4. Initial condition graphs for 3 permafrost region types from HBR and Polar Gas Pipeline reports (EBA Engineering Consultants Ltd., 1977; EBA Engineering Consultants Ltd., 1975).

3.3 Material Properties

3.3.1 Volumetric water content

The gravimetric water content values for each soil type were obtained from the HBR and Polar Gas Pipeline reports (EBA Engineering Consultants Ltd., 1977; EBA Engineering Consultants Ltd., 1975). In order to use this

data as input for TEMP/W, the gravimetric water content values were converted to volumetric water content using a formula developed by Andersland & Ladanyi (2004):

$$\theta = w(\frac{\rho_d}{\rho_w}) \quad [6]$$

which ρ_d is the dry density (kN/m^3) of soil, w is the gravimetric water content of soil and ρ_w is the density of water (kN/m^3). The dry density for each type of soil was derived from Andersland & Ladanyi (2004). Table 1 presents an overview of the gravimetric and volumetric water content for each type of soil in each station. The values provided correspond to the average water content derived from all the boreholes for a particular material.

Table 1: Gravimetric and volumetric water content values used in the thermal modeling.

	Continuous	
	Gravimetric water content (%)	Vol. water content
Sand	17.48	0.32
Silty Sand	18.89	0.36
Silt	12.18	0.19
Silty Clay	17.63	0.36
Clay	30	0.49
	Extensive discontinuous	
Sand	11.45	0.2
Silty Sand	30.88	0.59
Silt	22.92	0.35
Silty Clay	37.59	0.76
Clay	46.8	0.7
	Sporadic discontinuous	
Sand	24.3	0.44
Silty Sand	10.5	0.2
Silt	20.6	0.32
Silty Clay	42.61	0.86
Clay	43.87	0.72

3.3.2 Unfrozen water content

Unfrozen water content is a critical factor in the thermal behavior of frozen soils, particularly for fine-grained soils where some water remains unfrozen at negative temperatures. This water is adsorbed around clay particles and its amount increases with the specific surface area of the clay particles (Farouki, 1985). The unfrozen water content is essential in the process of water migration to the freezing zone and improving the thermal contact between the soil matrix and ice. Previous research has shown that the unfrozen water content is related to specific surface area and temperature (Andersland & Ladanyi, 2004). In this study, the unfrozen water content functions in the models were based on the default graphs provided by the GeoStudio software (GeoSlope, 2021).

3.3.3 Heat capacity

Heat capacity is defined as the amount of heat required to raise the temperature of a unit mass of a substance by one degree Celsius. The values for heat capacity used in the analysis were derived from Andersland & Ladanyi (2004) and are presented in **Error! Reference source not found.**.

Table 2: Frozen and unfrozen heat capacity values for different types of soils used in this study (Andersland & Ladanyi, 2004).

	Frozen Vol. Heat Capacity (kJ/m^3/ºC)	Unfrozen Vol. Heat Capacity (kJ/m^3/ºC)
Sand	2000	2750
Silty Sand	2000	2775
Silt	2050	2800
Silty Clay	2000	2700
Clay	2000	2700

3.3.4 Thermal conductivity

Thermal conductivity (J/s/m/ºC) is a physical property that measures the ability of a material to conduct heat. The thermal conductivity of ice can be up to four times higher than that of liquid water (Andersland & Ladanyi, 2004), this value increases as the soil freezes and decreases as it thaws. The thermal conductivity of soil is also affected by its saturation and the amount and type of minerals present. However, since the mineral composition of the soils in this study is unknown, the frozen and unfrozen thermal conductivities were calculated using the values presented by Andersland & Ladanyi (2004). The graphs of the thermal conductivity in the Full Thermal mode in TEMP/W were then generated by the software. The values of frozen and unfrozen thermal conductivity used in this study are summarized in Table 3.

Table 3: Frozen and unfrozen thermal conductivity for different types of soils used in this study (Andersland & Ladanyi, 2004).

	Frozen Conductivity (J/s/m/ºC)	Unfrozen Conductivity (J/s/m/ºC)
Sand	2.25	1.63
Silty Sand	2.75	1.6
Silt	1.15	0.95
Silty Clay	1.15	0.95
Clay	1.15	0.95

4. SETTLEMENT CALCULATION METHOD

Ground settlement represents a critical factor within Civil Engineering infrastructures (Namadi et al., 2023). A type of ground settlement is thawing settlement that can occur due to the thawing of near-surface soil layers and the melting of excess ice. The resulting release of excess pore water causes strain, which can lead to a lowering of the ground surface (Motlagh et al., 2023). The amount of thaw settlement can be calculated using the following equation:

$$\delta = \varepsilon * \Delta ALT \quad [7]$$

where δ is the thaw settlement (m), ε is the thaw strain and ΔALT is the temporal change in active layer thickness (ALT) (m) derived from the thermal modeling results.

4.1 Thaw Strain

The calculation of thaw strain can be achieved through the application of an empirical relation, as established by several researchers (Hanna et al., 1978; Nelson et al., 1983; Speer et al., 1973; Crory, 1973). For this study, the graphs produced by Nelson et al. (1983) were utilized to determine the thaw strain. These graphs rely on the dry density of soils to predict the thaw strain. The values utilized for thaw strain in this study are compiled in Table 4.

Table 4: Thaw strain values for different types of soils used in this study (Andersland & Ladanyi, 2004; Nelson et al., 1983).

	Dry Density (kg/m^3)	Thaw Strain (%)
Sand	1810	3
Silty Sand	1920	3
Silt	1550	4
Silty Clay	2040	2
Clay	1650	5

5. THERMAL MODELING RESULTS

In this section of the study, the input parameters obtained from the HBR and Polar Gas reports were utilized to simulate soil columns, and the obtained results were presented as graphs showing changes in active layer thickness and resulting settlement for different soil types, regions, and scenarios (Figure 5).

The results presented in Figure 5 suggest that sporadic discontinuous regions along the HBR are highly susceptible to the impacts of climate warming in the majority of instances. Moreover, it is worth noting that certain data points are absent from the graphs, which indicate the disappearance of permafrost by that specific year. This occurrence is observed predominantly in sporadic discontinuous permafrost regions and RCP8.5 scenarios. Additionally, there is an increase in active layer changes from the Churchill to Sipiwesk Stations along the HBR, which can be attributed to the colder climate prevailing in the higher latitudes and the warmer temperatures present in the lower latitudes. Moreover, there are cases where the RCP4.5 scenario predicts greater settlement than RCP8.5, indicating uncertainty in different climate scenarios.

It should be noted that in some cases, a thin layer of seasonally frozen ground was observed to persist through the subsequent summer(s). In such cases, the depth of the seasonally frozen ground was not considered as the depth of active layer, and the second 0°C was considered as the depth of active layer.

6. DISCUSSION

Figure 6 displays the maximum and minimum changes in ALT in various soil types, where each minimum and maximum value corresponds to a specific RCP and permafrost region. The results indicate that silty sand and sand exhibit the highest changes in ALT, while silty clay shows the lowest changes. This suggests that locations along the HBR where silty sand is prevalent are more susceptible to ALT changes due to climate warming trends by 2070. Interestingly, not all minimum active layer thickness values occur in RCP2.6 in continuous permafrost and not all maximum active layer thickness values occur in RCP8.5 in sporadic discontinuous permafrost. RCP4.5 climate scenario or extensive discontinuous permafrost may also be the critical condition of the occurrence of such values. It is possible that the unexpected results observed in some scenarios could be due to extreme weather events or other factors that are not fully captured by the models used in the study. Climate models are based on a range of assumptions and simplifications, and uncertainties in the models can lead to discrepancies between predicted and actual outcomes. It is therefore important to continue improving and refining the models used to study climate change, as well as to conduct further research to better understand the complex interactions between different factors affecting permafrost and infrastructure stability.

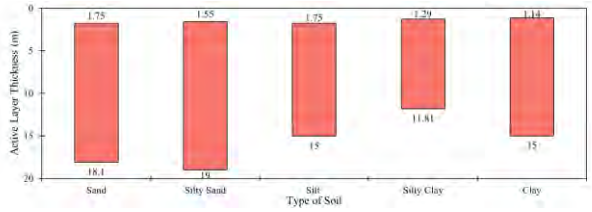

Figure 6: Maximum and minimum of ALT changes by year 2070 in different types of soils along the HBR. Silty sand and silty clay soils in this region showed the most and the least susceptibility, respectively, to warming trends by 2070.

Figure 7 illustrates the maximum and minimum settlements predicted in different soil types by 2070. The highest range of settlement belongs to clay soils, and the smallest range belongs to silty clay soils. These results are not entirely similar to the ALT changes (Figure 9) because of different thaw strain values for each soil type. Therefore, the dry density of soil also plays a critical role in measuring the susceptibility of the soil to climate warming trends.

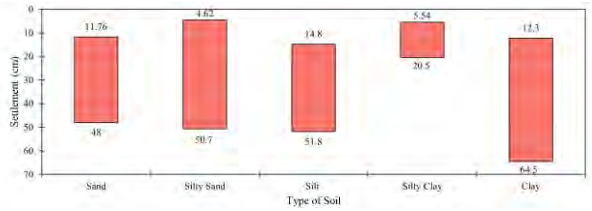

Figure 7: Maximum and minimum settlement by year 2070 in different types of soils along the HBR. Clay and silty clay soils in this region showed the most and the least susceptibility to warming trends by 2070.

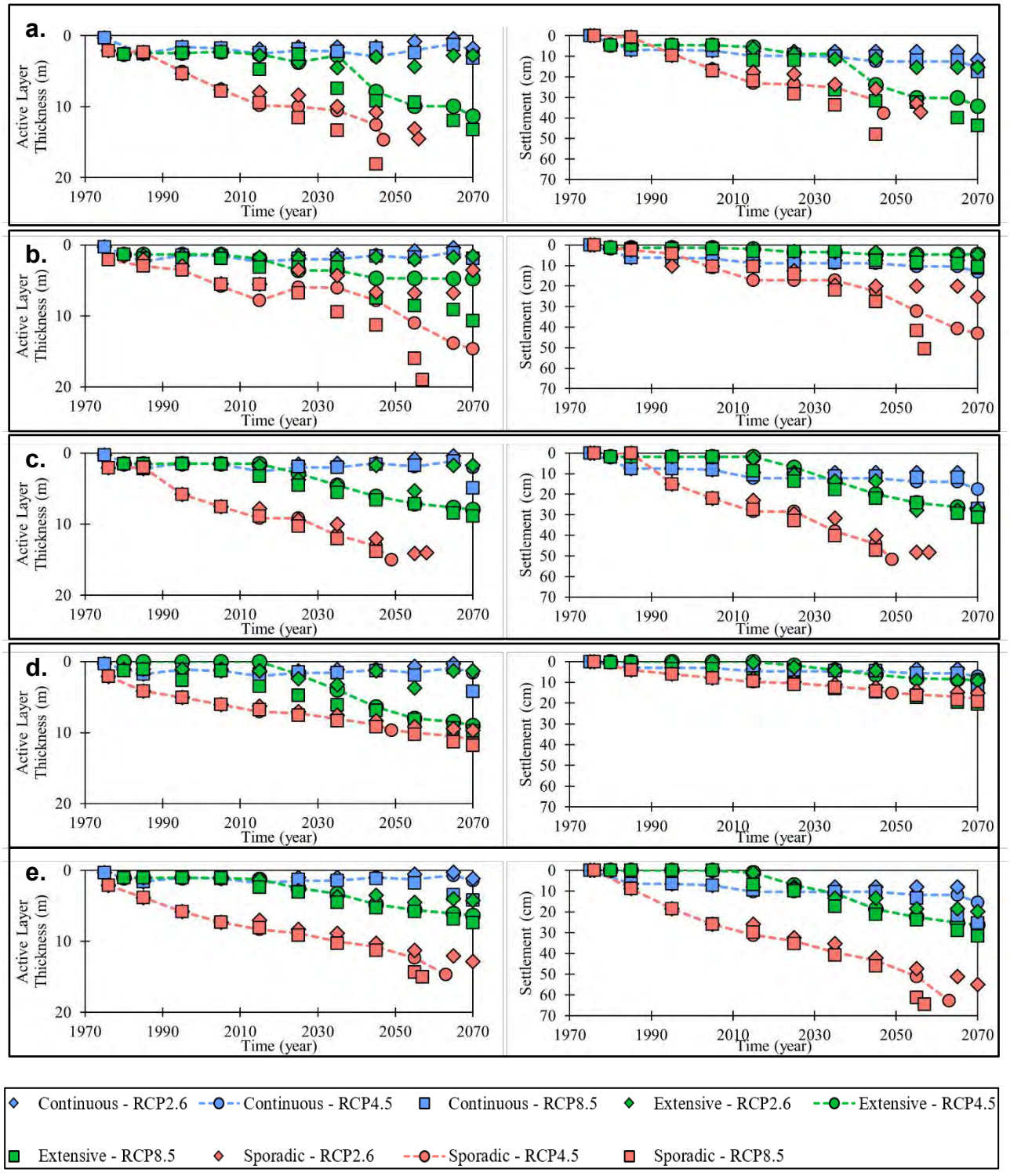

Figure 3: ALT and settlement results for typical soils found along the HBR for a. sandy, b. silty sand, c. silty, d. silty clay and e. clay soils. Water content for each soil type is based on average values in situ (Table 1).

7. CONCLUSION

In this study we analyzed the effects of critical parameters (i.e., soil type, climate scenario and permafrost coverage) on climate-driven permafrost thaw and settlement using the CMIP5 and TEMP/W software. Based on the analysis results, some conclusions were obtained as follows:

- The percentage of coverage of permafrost regions has a significant impact on the changes in

the ALT and settlement. The colder weather is prevalent in regions with greater permafrost coverage. Based on the findings of this study, greater settlement can be expected with increased permafrost coverage. Consequently, moving from north to south along the HBR, infrastructure is anticipated to experience more settlement by 2070.

- RCP8.5, the worst-case scenario in climate models, is expected to result in the most settlement compared to RCP2.6 and RCP4.5. However, in some cases, RCP4.5 predicts the most settlement, possibly due to extremes in the modeling period.

Future work could examine the thermal analysis probabilistically to predict the thaw settlement probability distribution in order to find the reliability of linear infrastructure built on permafrost regions. These steps could be conducted via a python interface. Also, multiple equations could be developed for predicting the thaw settlement in different types of soil using the probabilistic analysis.

8. ACKNOWLEDGEMENTS

In conducting this research, we are grateful for the funding provided by NSERC PermafrostNet. This research would not have been possible without their support. Dr. Teddi Herring has meticulously reviewed and provided insightful feedback on this manuscript, and we thank her for her time and effort. Research quality and rigor have been greatly enhanced by her invaluable contribution.

9. REFERENCES

Alfaro, M. C., Asce, A. M., Ciro, G. A., KENDALL; Thiessen, J.; Ng, T. (2009). Case Study of Degrading Permafrost beneath a Road Embankment. https://doi.org/10.1061/ASCE0887-381X200923:393.

Andersland, Orlando B. & Ladanyi, Branko. Frozen Ground Engineering Second Edition. The American Society of Civil Engineers & John Wiley & Sons, Inc, 2004.

Crory, F. E. (1973). Settlement associated with thawing permafrost. Permafrost: North American Contribution, 599–607.

Doré, G., Niu, F., & Brooks, H. (2016). ADAPTATION METHODS FOR TRANSPORTATION INFRASTRUCTURE BUILT ON DEGRADING PERMAFROST. PERMAFROST AND PERIGLACIAL PROCESSES, 27(4), 352–364.

EBA Engineering Consultants Ltd., (1975). “Hudson Bay Railway, Herchmer Subdivision, Bridge Crossing Evaluation”. Engineering Report Prepared for Canadian National Railways western region.

EBA Engineering Consultants Ltd., (1977). “Settlement of a Railway Embankment Constructed on Permafrost Peatlands”. Engineering Report Prepared for Canadian National Railways

Farouki, O. (1985). “Ground thermal properties.” Proc., Thermal Design Considerations in Frozen Ground Engineering, ASCE, New York, 186–203.

GEO-SLOPE. (2021). Heat and Mass Transfer Modeling with Geostudio, Calgary, AB, Canada.

Hajitaheriha, M. M., Akbarimehr, D., Hasani Motlagh, A., & Damerchilou, H. (2021). Bearing capacity improvement of shallow foundations using a trench filled with granular materials and reinforced with geogrids. *Arabian Journal of Geosciences*, *14*, 1-14. https://doi.org/10.1007/s12517-021-07679-y

Hanna, A. J., Saundersl, R. J., Leml, G. N., & CarLson, L. E. (1978). ALASKA HIGHWAY GAS PIPELINE PROJECT (YUKON) SECTION THAW SETTLEMENT DESIGN APPROACH

IPCC, 2014: Climate Change 2014: Synthesis Report. Contribution of Working Groups I, II and III to the Fifth Assessment Report of the Intergovernmental Panel on Climate Change [Core Writing Team, R.K. Pachauri and L.A. Meyer (eds.)]. IPCC, Geneva, Switzerland, 151 pp.

Lunardini, V. J. (1978). “Theory of N-factors and correlation of data.” Proc., 3rd Int. Conf. on Permafrost, National Research Council, Ottawa, Canada.

Motlagh, A. H., Hosseinzadeh, M., Hassanlourad, M., & Hamedsalman, M. (2023). Shear strength, adsorption, and microstructural behavior of sand-bentonite and sand-kaolinite mixtures contaminated with heavy metals. *Arabian Journal of Geosciences*, *16*(7), 1-22. https://doi.org/10.1007/s12517-023-11543-6

Namadi, A. H., Motlagh, A. H., Hassanlourad, M., & Hosseinzadeh, M. (2023). Impact of Heavy Metal and Carbonate on Geotechnical Properties of Sand-Bentonite Mixtures. *Indian Geotechnical Journal*, 1-11. https://doi.org/10.1007/s40098-023-00743-2

Nelson, R. A., Luscher’, U, Rooney’, J. W.; Stramler, A. A. (1983). Thaw strain data and thaw settlement predictions for Alaskan soils.

Prowse, T. D., Furgal, C., Melling, H., & Smith, S. L. (2009). Implications of climate change for northern Canada: The physical environment. Ambio, 38(5), 266–271. https://doi.org/10.1579/0044-7447-38.5.266

Roghani, A., & Eng NRC, P. (2021). Review of the current state of knowledge regarding the design, construction and maintenance of railway lines over permafrost.

Romanovsky, V. E., & Osterkamp, T. E. (1997). Thawing of the active layer on the coastal plain of the Alaska Arctic. Permafrost Periglacial Processes, 8, 1-22.

Ross, C., Siemens, G., & Beddoe, R. (2022). Initialization of thermal models in cold and warm permafrost. Arctic Science, 8(2), 362–394. https://doi.org/10.1139/as-2021-0013

Sadollahzadeh, B., Zakeri, J. A., Nouri Gheshlaghi, H., & Hasani Motlagh, A. (2021). Experimental and numerical assessment of the lateral resistance of ballasted railway track equipped with mid-winged sleeper. *Scientia Iranica*, *28*(5), 2546-2556.